

## Thermodynamic basis for a variational model for crystal growth

Bayard K. Johnson\* and Robert F. Sekerka  
*Carnegie Mellon University, Pittsburgh, Pennsylvania 15213*

Robert Almgren  
*University of Chicago, Chicago, Illinois 60637*  
 (Received 19 October 1998)

Variational models provide an alternative approach to standard sharp interface models for calculating the motion of phase boundaries during solidification. We present a correspondence between objective functions used in variational simulations and specific thermodynamic functions. We demonstrate that variational models with the proposed identification of variables are consistent with nonequilibrium thermodynamics. Variational models are derived for solidification of a pure material and then generalized to obtain a model for solidification of a binary alloy. Conservation laws for internal energy and chemical species and the law of local entropy production are expressed in integral form and used to develop variational principles in which a “free energy,” which includes an interfacial contribution, is shown to be a decreasing function of time. This free energy takes on its minimum value over any short time interval, subject to the laws of conservation of internal energy and chemical species. A variational simulation based on this model is described, and shown for small time intervals to provide the Gibbs-Thomson boundary condition at the solid-liquid interface. [S1063-651X(99)02307-7]

PACS number(s): 81.10.Aj, 05.70.Ln, 02.70.-c, 64.70.Dv

### I. INTRODUCTION

In computational modeling of crystal growth, standard sharp interface models are very cumbersome to solve numerically. This arises because the crystal-melt interface is a free boundary that must be tracked by some numerical algorithm with an accuracy necessary to compute its curvature, on which its local equilibrium conditions (temperature and composition) depend. Alternative models are being developed that are more efficient for numerical computations.

The phase-field model has received considerable attention because of its basis in the fundamental laws of irreversible thermodynamics, and because phase-field simulations can be used to compute crystal shapes quite complex in comparison with those obtained from numerical solutions to standard sharp interface models [1–6].

Variational models are another alternative. In variational models, one minimizes a “free energy,” subject to conservation conditions, to determine the position of the solid-liquid interface, and in a separate step solves the diffusion equation for temperature or chemical potential in the bulk. By iterating these two steps, one can compute the time evolution of a solid-liquid interface. Variational simulations for the solidification of a pure material were proposed and implemented by one of the present authors [7] Roosen and Taylor [8] and Taylor [9–11] used similar principles to develop simulations of the evolution of interfaces with crystal-line (faceted) surface energies. These simulations were based on a mathematical connection to standard sharp interface models. In this paper, a thermodynamic basis for variational models is presented and generalized to include alloy solidification.

Variational simulations are well suited to massively parallel computation and do not require such careful tracking of the interface as one would need for sharp interface models to compute the interface curvature by some combination of local curve fitting and interpolation. An advantage of variational simulations from a theoretical standpoint is that the Gibbs-Thomson interfacial boundary condition results directly from the minimization of a free energy, which is its underlying basis.

We derive variational models for the solidification of a pure material and the solidification of a binary alloy. Two versions of the variational model are derived in each case: a quadratic and a linear model.

#### A. Some notation

Consider a volume occupied by two phases (e.g., a solid crystal and its liquid melt) separated by an interface. We treat a subvolume  $V$  contained within a surface  $A_{\text{out}}$  that may include a portion of the interface. The intersections of the solid, liquid, and interface with  $V$  are called  $V_S$ ,  $V_L$ , and  $A_{SL}$ , respectively.

A dimensionless potential field  $u$  represents a temperature field in the case of a pure substance and a chemical potential field in the case of a binary alloy. In the variational models and in the standard sharp interface models,  $u$  is a solution of the diffusion equation,

$$\dot{u} = \nabla^2 u, \quad (1)$$

in the bulk solid and liquid. The dot above a variable denotes partial differentiation with respect to dimensionless time.

Later we consider a coordinate system that is moving in the  $z$  direction with nondimensional speed 1 with respect to the crystal, in which case the bulk fields obey a diffusion equation of the form

\*Present address: MEMC Electronic Materials Inc., Saint Peters, MO 63376.

$$\dot{u} = \nabla^2 u + \frac{\partial u}{\partial z}. \quad (2)$$

For both the variational models and standard sharp interface models, the bulk fields are determined by a solution of the diffusion equation, but the models differ in the way that the boundary conditions at the crystal-melt interface are treated.

### B. Standard sharp interface models

In standard sharp interface models,  $u$  is continuous at the solid-liquid interface and takes on the value

$$u - \bar{u} = -(f^{xs} + f_{\theta\theta}^{xs})K, \quad (3)$$

where  $\bar{u}$  is a reference potential that can frequently be taken to be zero,  $f^{xs}$  is proportional to an excess interfacial free energy, and  $K$  is the dimensionless curvature of the interface. Since  $f^{xs}$  is assumed to depend on the surface orientation, the notation  $(f^{xs} + f_{\theta\theta}^{xs})K$ , which would be correct in two dimensions, is a symbolic representation for  $(f^{xs} + f_{\theta_1\theta_1}^{xs})K_1 + (f^{xs} + f_{\theta_2\theta_2}^{xs})K_2$ , which applies in three dimensions. The  $\theta$  subscripts represent differentiation of  $f$  with respect to  $\theta$ , and the subscripts 1 and 2 identify angles between the normal and the two principal axes of curvature for the interface. Equation (3) is often referred to as the Gibbs-Thomson equation.

There is also a conservation condition at the crystal-melt interface of the form

$$V_n = [\nabla u^S - \nabla u^L] \cdot \mathbf{n}, \quad (4)$$

where  $V_n$  is the dimensionless local normal growth speed, and  $\mathbf{n}$  is the normal to the interface pointing into the liquid. Equation (4) applies when the thermal conductivities in solid and liquid are equal, which is an approximation we discuss later.

Equation (1) or (2), subject to the boundary conditions (3) and (4) on  $A_{SL}$  with Neumann, Dirichlet, or other suitable conditions on the external boundary, constitute a mathematically well-posed model for the evolution of crystal shapes.

### C. Variational models

In variational models, the process of determining the evolution the interface position and potential field over a short time interval from  $t$  to  $t + \Delta t$ , is divided into two computational steps: (i) bulk diffusion and (ii) interface motion. The potential field (e.g., temperature for solidification of a pure material) can change during both steps.

In the first step, the bulk fields are computed by allowing heat to diffuse for time  $\Delta t$  without regard to the presence of a solid-liquid interface, and the interface position does not change. In the second step, the interface can change position. The bulk field changes in the second step only to account for the change in potential due to motion of the interface (e.g., to account for latent heat in the case of a pure material). The flux of potential associated with the motion of the interface is called the difference flux, because it results from a difference between solid and liquid equilibrium values of a conserved quantity, such as internal energy.

In the second step, the new interface position is found by the minimization of a total energy,  $\mathcal{F}$  of the form

$$\mathcal{F} = \int_V f dV + \int_{A_{S,L}} f^{xs} dA, \quad (5)$$

which is minimized over all possible new interface configurations, subject to a conservation constraint. The quantity  $f$  is a dimensionless bulk energy density that is a specified function of the potential field  $u$ , and  $f^{xs}$  is a dimensionless free-energy density of the crystal-melt interface, and can depend on its orientation.

The difference flux plays an important role in the minimization of  $\mathcal{F}$ . At the beginning of an iteration step, the bulk field and the interface position are in a configuration we will call  $A$ . After the bulk diffusion step (step 1) has been completed, the system is in configuration  $B$ , which has interface position and configuration corresponding to  $A$  but a new potential field *due to diffusion for a time  $\Delta t$* . Configuration  $B$  is, therefore, an intermediate configuration not necessarily representing the physical system configuration at any time. To obtain the actual configuration  $C$  one must minimize  $\mathcal{F}$  with respect to all interface positions and configurations. During the minimizing process, one might try configuration  $B'$  that differs from configuration  $B$  in the location of the interface, and in the potential field. The potential field for  $B'$  is the sum of the potential field associated with configuration  $B$  and the new potential associated with the difference flux. The new potential is determined by taking each volume element that would change phase if the system were to evolve from  $B$  to  $B'$  and distributing the released potential (or withdrawing the absorbed potential in the case of melting) in a small neighborhood of approximate dimensionless radius  $\sqrt{\Delta t}$  of all volume elements that have changed phase. Thus any volume that changes phase can only affect the bulk potential in a local neighborhood whose size is determined by  $\Delta t$ . By distributing potential in a small but finite neighborhood of material that has changed phase, one accounts for the diffusion that would take place between the time of the phase transformation, assumed to be intermediate to  $t$  and  $t + \Delta t$ , and the end of the time step at  $t + \Delta t$ . After determining configuration  $B'$  (interface position and new bulk field), one can compute  $\mathcal{F}$  for  $B'$ , and compare it with that for  $B$ . By trying a large number of possible interface configurations, one can find that configuration that minimizes  $\mathcal{F}$ , and take that as the updated system configuration  $C$  at time  $t + \Delta t$ . This configuration will be configuration  $A$  for the next iteration.

Several variational models, for which  $f$  depends on  $u$  in various ways, are described in this paper. The derivations presented below treat only the variational step (step 2) of the algorithm discussed above. For each model, the law of positive local entropy production and conservation laws (for internal energy and/or chemical species) are used to show that

$$\partial \mathcal{F} / \partial t \leq 0. \quad (6)$$

The conservation condition that we will apply to step 2 is used to determine the difference flux and can be expressed in the form

$$\int_{A_{S,L}} V_n dA = \int_V \dot{u} dV, \quad (7)$$

where  $V_n$  is the normal growth speed of the interface, and results from a statement of conservation of the quantity for which  $u$  is the conjugate potential. For example, if  $u$  is a dimensionless temperature, the conservation condition is a statement of the conservation of energy accounting for the latent heat of solidification.

A variational model in the limit  $\Delta t \rightarrow 0$  and a standard sharp interface model will both impose the Gibbs-Thomson boundary condition for  $u$  at the crystal-melt interface.

#### D. Approximations

It is assumed that the materials being modeled are rigid and of constant density, so that transport is purely diffusive (i.e., no convection). We adopt a symmetric model, for which the appropriate transport coefficients in solid and liquid are equal, which greatly simplifies the calculations and is essential for the derivation of the variational model. For the solidification of a pure material, the thermal diffusion coefficients in solid and liquid can be of comparable magnitude, but are usually not equal. For metals, they differ typically by a factor of 2, and for ice and water by approximately 3 [12]. For chemical diffusion in a binary mixture, the diffusion coefficient in the solid is typically three or four orders of magnitude smaller than that in the liquid, so the assumption of equal diffusion coefficients is incorrect for this case. A more appropriate approximation would be to assume that the diffusion coefficient in the solid is zero.

There exist systems for which the diffusion coefficients in solid and liquid are comparable, and to which the mathematical formulation presented in Sec. III may be applied. In the experimental work of Melo and Oswald [13], in which they study the directional growth of a liquid crystal phase into another one, the diffusion coefficients in the two phases differ by roughly a factor of 2.

Another consideration is the relative importance of the transport coefficient in the solid to the overall behavior of some systems. For a pure material growing freely into a supercooled liquid, one can argue that the solid is nearly isothermal because the temperature gradients that occur in the solid are due solely to the effects of capillarity on the interfacial temperature. Almost independent of what value one chooses for the thermal conductivity in the solid, most of the heat transport that leads to growth comes from the much larger temperature gradients in the liquid. The choice of thermal diffusion coefficient for the solid in such cases would not dramatically affect the behavior of the system. By the same argument, choosing a finite diffusion coefficient in solid should not give rise to significant material fluxes, provided that the gradients in solid are small compared to those in the liquid.

Although the approximation of equal transport coefficients in solid and liquid limit the applicability of the model, we claim that one can obtain some meaningful insight into the process of crystal growth, and proceed with these issues in mind.

## II. SOLIDIFICATION OF A PURE MATERIAL

We first treat a variational model of solidification of a pure material from its melt in the absence of convection. Derivations that use the same basic laws can be used to ob-

tain standard sharp interface models [14–16].

#### A. Energy conservation and entropy production

The law of conservation of energy can be expressed in the form

$$\frac{d}{dt} \left[ \int_{V_S} e^S dV + \int_{V_L} e^L dV + \int_{A_{SL}} e^{xs} dA \right] = - \int_{A_{out}} \mathbf{j}_e \cdot \mathbf{n}_{out} dA, \quad (8)$$

where  $e$  is the internal energy density,  $\mathbf{j}_e$  is the internal energy flux, and  $\mathbf{n}_{out}$  is the outward pointing normal to  $A_{out}$ . The superscripts  $S$ ,  $L$ , and  $xs$  hereafter denote, respectively, the solid, liquid, and surface excess of the quantity.

Equation (8) can be rewritten by applying the time derivative on the left-hand side to obtain

$$\begin{aligned} & \int_{V_S} \dot{e}^S dV + \int_{V_L} \dot{e}^L dV + \int_{A_{SL}} (e^S - e^L) V_n dA \\ & + \int_{A_{SL}} (e^{xs} + e_{\theta\theta}^{xs}) K V_n dA + \int_{A_{SL}} \dot{e}^{xs} dA \\ & = - \int_{A_{out}} \mathbf{j}_e \cdot \mathbf{n}_{out} dA, \end{aligned} \quad (9)$$

where  $K$  is the interfacial curvature, and the dot ( $\dot{\phantom{x}}$ ) above a variable represents partial differentiation with respect to time. The excess internal energy density may be a function of the orientation of the interface, and may depend explicitly on time.

In bulk solid or bulk liquid (no  $A_{SL}$ ), Eq. (9) can be reduced to differential form by using the divergence theorem on the right-hand side and shrinking  $V$  to a point, resulting in

$$\dot{e} = - \nabla \cdot \mathbf{j}_e. \quad (10)$$

If, instead, one shrinks  $V$  to a portion of the interface, then shrinks that interfacial area to a point, the conservation condition becomes

$$(e^S - e^L) V_n + (e^{xs} + e_{\theta\theta}^{xs}) K V_n + \dot{e}^{xs} = [\mathbf{j}_e^S - \mathbf{j}_e^L] \cdot \mathbf{n}, \quad (11)$$

where  $\mathbf{n}$  is the unit normal to  $A_{SL}$  pointing into the liquid, and  $\mathbf{j}_e^S$  and  $\mathbf{j}_e^L$  are the internal energy fluxes in the solid and liquid, respectively.

The second law of thermodynamics (positive local entropy production) for this system can be written

$$\begin{aligned} & \frac{d}{dt} \left[ \int_{V_S} s^S dV + \int_{V_L} s^L dV + \int_{A_{SL}} s^{xs} dA \right] \\ & = - \int_{A_{out}} \mathbf{j}_s \cdot \mathbf{n}_{out} dA + \int_V \tilde{s}_I dV + \int_{A_{SL}} \tilde{s}_I^{xs} dA, \end{aligned} \quad (12)$$

where  $s$  is the entropy density,  $\mathbf{j}_s$  is the entropy flux,  $\tilde{s}_I$  and  $\tilde{s}_I^{xs}$  are the local rates of entropy production per unit volume in the bulk, and on the interface, respectively. These quantities must always satisfy  $\tilde{s}_I \geq 0$  and  $\tilde{s}_I^{xs} \geq 0$ , where the equal sign applies only to a hypothetical reversible process.

By applying the time derivative on the left-hand side of Eq. (12) one obtains

$$\begin{aligned} & \int_{V_S} \dot{s}^S dV + \int_{V_L} \dot{s}^L dV + \int_{A_{SL}} (s^S - s^L) V_n dA \\ & + \int_{A_{SL}} (s^{xs} + s_{\theta\theta}^{xs}) K V_n dA + \int_{A_{SL}} \dot{s}^{xs} dA \\ & = - \int_{A_{out}} \mathbf{j}_s \cdot \mathbf{n}_{out} dA + \int_V \dot{\tilde{s}}_I dV + \int_{A_{SL}} \dot{\tilde{s}}_I^{xs} dA. \end{aligned} \quad (13)$$

Equation (12) can also be reduced in bulk to an equation which is similar to Eq. (10) with an extra entropy production term,

$$\dot{s} = -\nabla \cdot \mathbf{j}_s + \tilde{s}_I, \quad (14)$$

and on the interface,

$$(s^S - s^L) V_n + (s^{xs} + s_{\theta\theta}^{xs}) K V_n + \dot{s}^{xs} = [\mathbf{j}_s^S - \mathbf{j}_s^L] \cdot \mathbf{n} + \tilde{s}_I^{xs}. \quad (15)$$

### B. Variational models

The variational models to be derived here for the pure material were proposed previously [7] and motivated intuitively based on the mathematical structure of the problem.

If the heat capacities per unit volume  $c_v$  in the solid and in the liquid are assumed to be equal and independent of the temperature, then the internal energy density

$$e^{S,L} = c_v (T - T_m) + e_0^{S,L}, \quad (16)$$

where the quantities  $e_0^{S,L}$  are constants for which  $e_0^L - e_0^S = L_v$ , where  $L_v$  is the latent heat of fusion per unit volume. Because  $de = Tds$ , one can write

$$s^{S,L} = c_v \ln(T/T_m) + s_0^{S,L}, \quad (17)$$

where  $s_0^{S,L}$  are constants for which  $s_0^L - s_0^S = L_v/T_m$ .

#### 1. Quadratic objective function

Consider a free-energy density defined by  $\tilde{f}_m = e - T_m s$ , which differs from the Helmholtz free-energy density,  $\tilde{f} = e - Ts$ , in that the temperature that multiplies the entropy is constant, the melting temperature for a planar interface. The surface excess of this energy is simply  $\tilde{f}_m^{xs} = e^{xs} - T_m s^{xs}$ .

By expanding  $\tilde{f}_m(T)$  about  $T_m$ , one finds to second order,

$$\begin{aligned} \tilde{f}_m(T) &= \tilde{f}_m(T_m) + \left. \frac{\partial \tilde{f}_m}{\partial T} \right|_{T_m} (T - T_m) + \frac{1}{2} \left. \frac{\partial^2 \tilde{f}_m}{\partial T^2} \right|_{T_m} (T - T_m)^2 \\ &+ \dots \end{aligned} \quad (18)$$

The first term in the expansion is the Helmholtz free energy at the melting temperature. The second term is zero, because  $de = Tds$ , and because the derivative is evaluated at  $T_m$ . The third term can be evaluated and is found to be

$$\frac{c_v}{2T_m} (T - T_m)^2. \quad (19)$$

Since  $\tilde{f}_m(T_m)$  and  $c_v$  are independent of phase,  $\tilde{f}_m$  is independent of phase at any given value of  $T$ .

Next, consider the thermodynamic laws. Multiplying Eq. (12) by  $T_m$ , subtracting that product from Eq. (8), and using  $\mathbf{j}_e = T \mathbf{j}_s$ , one obtains

$$\begin{aligned} \frac{d}{dt} \left[ \int_V \tilde{f}_m dV + \int_{A_{S,L}} \tilde{f}_m^{xs} dA \right] &= - \int_{A_{out}} \left( 1 - \frac{T_m}{T} \right) \mathbf{j}_e \cdot \mathbf{n} dA \\ &- T_m \left[ \int_V \dot{\tilde{s}}_I dV + \int_{A_{SL}} \dot{\tilde{s}}_I^{xs} dA \right], \end{aligned} \quad (20)$$

where  $V = V_S + V_L$ .

For a perturbation of a small portion of the solid-liquid interface, the surface  $A_{out}$  may be placed far enough away that the difference flux from the motion of  $A_{SL}$  will not reach  $A_{out}$  in a short time interval  $\Delta t$ , leading to  $\mathbf{j}_e \cdot \mathbf{n} = \mathbf{0}$  on  $A_{out}$ . By applying Eq. (20) over a small time interval  $\Delta t$  and to a small volume  $V$  that, however, is sufficiently large that  $\mathbf{j}_e \cdot \mathbf{n} = \mathbf{0}$  on  $A_{out}$  substituting the nondimensionalized temperature,  $u = (T - T_m)/(L_v/c_v)$ , using the expanded  $\tilde{f}_m$  from Eq. (18) and keeping terms to second order in  $u$ , Eq. (20) becomes

$$\begin{aligned} \frac{d}{dt} \left\{ \int_V \frac{1}{2} u^2 dV + \int_{A_{SL}} \frac{\tilde{f}_m^{xs}}{\mathcal{E}} dA \right\} \\ = - \frac{T_m}{\mathcal{E}} \left\{ \int_V \dot{\tilde{s}}_I dV + \int_{A_{SL}} \dot{\tilde{s}}_I^{xs} dA \right\}, \end{aligned} \quad (21)$$

where the energy density parameter is  $\mathcal{E} = L_v^2/(c_v T_m)$ , and where length variables have been rescaled by a characteristic length  $l$  and time by  $l^2/\kappa$ , where  $\kappa$  is the thermal diffusion coefficient.

Substituting Eq. (16) into Eq. (9), assuming that  $\mathbf{j}_e = \mathbf{0}$  on  $A_{out}$  and neglecting the terms containing  $e^{xs} + e_{\theta\theta}^{xs}$  and  $\dot{e}^{xs}$  because  $(e^{xs} + e_{\theta\theta}^{xs})K \ll L_v$  and  $\dot{e}^{xs}/V_n \ll L_v$ , one obtains

$$\int_V \dot{u} dV - \int_{A_{SL}} V_n dA = 0. \quad (22)$$

By defining the objective function  $f = u^2/2$  and  $f^{xs} = \tilde{f}_m^{xs}/\mathcal{E}$ , Eqs. (21) and (22) can be rewritten in the form of Eqs. (6) and (7), respectively. In addition, the bulk  $u$  fields must satisfy the diffusion equation (1). Therefore, a model based on Eqs. (6), (7), and (1) is consistent with the first and second laws of thermodynamics.

#### 2. Linear objective function

In this alternative variational formulation, an objective function  $f$  that has a different dependence on  $u$  is defined. Using Eqs. (16) and (17), one can write

$$\tilde{f}^S - \tilde{f}^L = [(T/T_m) - 1] L_v = u \mathcal{E}, \quad (23)$$

where  $\tilde{f} = e - Ts$  is the true Helmholtz free energy, and  $u$  and  $\mathcal{E}$  are given in the previous section.

Multiplying Eq. (15) by  $T$  and subtracting the product from Eq. (11), then integrating the result over a portion of the interface, one obtains

$$\int_{A_{SL}} \left\{ uV_n + \frac{\tilde{f}^{xs} + \tilde{f}_{\theta\theta}^{xs}}{\mathcal{E}} KV_n \right\} dA = -\frac{1}{\mathcal{E}} \int_{A_{SL}} T\tilde{s}_I^{xs} dA, \quad (24)$$

where  $\tilde{f}^{xs} = (e^{xs} - Ts^{xs})$  is the surface excess Helmholtz free energy, which is assumed not to depend explicitly on time.

Consider an objective function

$$f = \begin{cases} u/2 & \text{in solid} \\ -u/2 & \text{in liquid.} \end{cases} \quad (25)$$

One can write

$$\frac{d}{dt} \int_V f dV = \int_V \frac{\partial f}{\partial t} dV + \int_{A_{SL}} uV_n dA.$$

Substituting this into Eq. (24), and recalling that  $\tilde{s}_I^{xs} \geq 0$ , one finds

$$\frac{d}{dt} \left[ \int_V f dV + \int_{A_{SL}} \frac{\tilde{f}^{xs}}{\mathcal{E}} dA \right] + \frac{1}{2} \left[ \int_{V_L} \dot{u} dV - \int_{V_S} \dot{u} dV \right] \leq 0, \quad (26)$$

where the time derivative of  $\tilde{f}^{xs}$  was moved outside of the integral in the second term of Eq. (24) to obtain Eq. (26) [14].

Because the latent heat is distributed isotropically (a direct result of the assumption of equal transport coefficients in solid and liquid), the third and fourth terms on the left-hand side of Eq. (26) reduce approximately to a constant times the difference in volumes occupied by solid and liquid in the region  $V$ . Assuming  $V$  is a sphere of small radius  $r_h$ , the fractional difference in volume between solid and liquid is proportional to  $r_h K$ . By choosing  $r_h \ll R$ , where  $R$  is the radius of curvature of the interface, one can neglect the sum of the third and fourth terms in Eq. (26) [7]. Setting the sum of these terms equal to zero is equivalent to assuming that the conjugate variable (energy) associated with the potential  $u$  released because of the phase transformation is approximately equally distributed between the solid and liquid. Thus we obtain the approximate inequality,

$$\frac{d}{dt} \left[ \int_V f dV + \int_{A_{SL}} \frac{\tilde{f}^{xs}}{\mathcal{E}} dA \right] \leq 0. \quad (27)$$

Using the same nondimensionalization of the position and time variables that was used for the quadratic case, Eq. (26) takes the form of Eq. (6) where  $f$  is given by Eq. (25), and  $f^{xs} = \tilde{f}^{xs}/\mathcal{E}$ . The minimization in the linear case is also subject to the constraint of energy conservation, Eq. (7).

### C. Global behavior of $\tilde{f}$ and $\tilde{f}_m$

We have identified thermodynamic quantities  $\mathcal{F}$  that decrease monotonically subject to the constraint of energy con-

servation. Whether such a quantity decreases globally for the *entire* variational algorithm for a *thermally insulated system* depends on how  $\mathcal{F}$  behaves when the potential field diffuses. Existence of a quantity that decreases globally in time has certain theoretical advantages [17], though it is not necessary for practical computations.

To understand this, we return to the variational algorithm presented in the Introduction. At the end of step 1, the intermediate configuration is  $B$  and has the same interface geometry as  $A$ , but differs by diffusion of the potential. In the minimization step, we consider a variety of configurations  $B'$  in an attempt to minimize  $\mathcal{F}$ . Let  $C$  be the final minimizing configuration. Now, since  $B$  is one of the candidate minimizers in step 2, we certainly have  $\mathcal{F}(C) \leq \mathcal{F}(B)$ . We shall call  $\mathcal{F}$  a *global decreaser* if we can guarantee that  $\mathcal{F}(C) \leq \mathcal{F}(A)$ ; that is, if  $\mathcal{F}$  necessarily decreases from one time step to the next. Clearly, this will be the case if  $\mathcal{F}$  is decreased in the diffusion step of the algorithm, for then we have  $\mathcal{F}(B) \leq \mathcal{F}(A)$  and  $\mathcal{F}$  is a global decreaser.

Negative entropy, for example, is a global decreaser. Note that the entropy of bulk solid or liquid is a concave downward function of the internal energy, and hence the temperature, for constant specific heat, which we have assumed. Thermal diffusion drives an insulated system toward a system average temperature and the total integrated entropy to larger values. Negative entropy is also a global decreaser when multiple phases are considered. The disadvantage of the entropy in the context of variational algorithms is that it is not continuous at the solid-liquid interface.

The Helmholtz free energy is not a global decreaser, and neither is the linear objective function derived from it. This is why we have introduced the objective function  $\tilde{f}_m$ , which is a global decreaser, and which is continuous at the solid-liquid interface; the quadratic functional derived from  $\tilde{f}_m$  inherits these characteristics.

## III. SOLIDIFICATION OF A BINARY ALLOY

We develop our variational model of solidification of a binary alloy by adding the conservation of material species to the previous laws. This model is also applicable to the isothermal precipitation of a crystal with different composition from that of the solution from which it grows.

### A. Material conservation

The law of conservation of material is

$$\frac{d}{dt} \left[ \int_{V_S} c_i^S dV + \int_{V_L} c_i^L dV + \int_{A_{SL}} c_i^{xs} dA \right] = - \int_{A_{out}} \mathbf{j}_i \cdot \mathbf{n}_{out} dA, \quad (28)$$

where  $c_i$  is the local concentration (number per unit volume) of species  $i$ , and  $\mathbf{j}_i$  is the local flux of species  $i$ . The subscripts  $i$  allow for several species, each of which must obey Eq. (28). Fluxes are measured with respect to the center of moles reference frame. It is assumed that the total concentration  $\sum_i c_i$  is constant and uniform; therefore, the center of moles reference frame is the same as the frame in which the solid is at rest.

Equation (28) reduces in bulk to

$$c_i^{S,L} = -\nabla \cdot \mathbf{j}_i \quad (29)$$

and on the interface to

$$(c_i^S - c_i^L)V_n + c_i^{xs}KV_n = [\mathbf{j}_i^S - \mathbf{j}_i^L] \cdot \mathbf{n}. \quad (30)$$

Hereafter, the specific case of two species, labeled 1 and 2, is treated. It is assumed that the total concentration ( $c_1 + c_2$ ) is constant and uniform in both phases; therefore,  $dc_1 = -dc_2$  and  $\mathbf{j}_1 = -\mathbf{j}_2$  in either phase. Identification of the interface position with the equimolar surface for species 1 provides  $c_1^{xs} = 0$ . Because  $(c_1 + c_2)$  is constant, the equimolar surface for species 1 is also the equimolar surface for species 2, and, therefore,  $c_2^{xs} = 0$ . Because any variation in  $c_2$  brings about a related change in  $c_1$ , it suffices to track  $c_2$  alone. Equation (29) can be written for *either* species 1 or 2 in bulk solid or liquid in the form

$$\dot{c} = -\nabla \cdot \mathbf{j}, \quad (31)$$

and Eq. (30) becomes

$$(c^S - c^L)V_n = [\mathbf{j}^S - \mathbf{j}^L] \cdot \mathbf{n}, \quad (32)$$

where  $c = c_2$  and  $\mathbf{j} = \mathbf{j}_2$ .

We adopt a model similar to that proposed by Langer [18] for directional solidification for which the concentration vs chemical potential curves have the same slope in both phases. Consider a portion of the phase diagram for which  $c^L - c^S \equiv \Delta c_0$  is constant. The miscibility gap is usually not constant, but over a certain range of concentrations, and for some materials, this is a reasonable approximation. We also assume that the effective chemical potential,  $\mu \equiv \mu_2 - \mu_1$ , is a linear function of  $c$  in both solid and liquid, where  $\mu_1$  and  $\mu_2$  are the chemical potentials of species 1 and 2, respectively. One can then write

$$c^{S,L} = b(\mu - \mu_0) + c_0^{S,L}, \quad (33)$$

where  $c_0^S$  and  $c_0^L$  are constants with difference  $\Delta c_0 = c_0^S - c_0^L$ ,  $b$  is a constant slope, and  $\mu_0$  is the effective chemical potential of the liquid at  $T_0$  and  $c_0^L$ . A compatible form for the  $\mu$ 's as a function of  $c$  and  $T$  is

$$\begin{aligned} \mu_1^S &= \eta(c^S, T), \\ \mu_1^L &= \lambda(c^L, T), \\ \mu_2^S &= \eta(c^S, T) + \frac{1}{b}(c^S - c_0^S), \\ \mu_2^L &= \lambda(c^L, T) + \frac{1}{b}(c^L - c_0^L), \end{aligned} \quad (34)$$

where  $\eta$  and  $\lambda$  are functions of  $c$  and  $T$ .

Along the coexistence curve, chemical potentials for each species are equal,

$$\mu_1^S = \mu_1^L, \quad \mu_2^S = \mu_2^L, \quad (35)$$

leading to two equations for the equilibrium values,  $c^{S*}$  and  $c^{L*}$ , where the star (\*) denotes the value of  $c^S$  or  $c^L$  on the coexistence curve. One can solve these equations to find  $(c^{L*} - c^{S*}) = \Delta c_0$ . One also obtains the equation

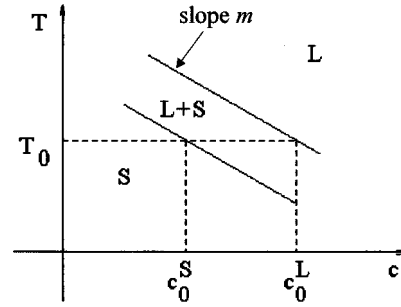


FIG. 1. Phase diagram. The concentrations at the coexistence point are linear functions of the temperature. The reference temperature  $T_0$  locates the values of  $c_0^S$  and  $c_0^L$ . The slope  $m$  in this case is negative.

$$\eta(c^{L*} - \Delta c_0, T) = \lambda(c^{L*}, T), \quad (36)$$

which is the general equation for the liquidus line. The solidus line is shifted exactly  $\Delta c_0$  from the liquidus line. Although this cannot be true in general, and is not true in the dilute limit (as  $c_1$  approaches 0, for example), it can be true for some range of values of  $c$ . We choose to work within that range.

We assume that the liquidus curve is a straight line: take the form

$$c^{L*} = c_0^L + (T - T_0)/m, \quad (37)$$

where  $T_0$  is a constant temperature,  $m$  is a constant liquidus slope, and  $c_0^L$  is the equilibrium concentration corresponding to the temperature  $T_0$ . Figure 1 is a sketch of the phase diagram for this model.

## B. Variational models

The variational model will incorporate an expanded version of the Gibbs-Thomson equation that includes the effects of the local composition on the melting point. Both quadratic and linear models will be developed. The reader is referred to the literature for derivations of the corresponding standard sharp interface models [14,16,19].

We use the Kramers free energy (per unit volume)

$$\omega := e - Ts - \mu_i c_i, \quad (38)$$

where a summation over  $i$  is implied. In the case of a pure substance,  $\omega$  is simply the negative of the pressure. The surface excess, per unit area, of the extensive counterpart to  $\omega$  is the surface tension for a binary alloy.

### 1. Quadratic objective function

Consider the energy  $\omega_0 = e - T_0 s - \mu_{0i} c_i$ , which differs from the Kramers free energy in that the temperature that multiplies the entropy and the chemical potentials that multiply the concentrations are constant. The surface excess of this energy is simply  $\omega_0^{xs} = e^{xs} - T_0 s^{xs} - \mu_{0i} c_i^{xs}$ . The function  $\omega_0$  will be regarded to be a function of  $T$  and the  $\mu_i$ . It is assumed that the temperature differs from  $T_0$  by a small amount  $\Delta T$ , and that the chemical potentials  $\mu_i$  differ from  $\mu_{0i}$  by small amounts  $\Delta \mu_i$ . Expanding  $\omega_0$  about  $T_0$ ,  $\mu_{01}$ , and  $\mu_{02}$ , one finds

$$\begin{aligned}
\omega_0(T, \mu_1, \mu_2) = & \omega_{00} + \frac{\partial \omega_0}{\partial T} \Big|_0 \Delta T + \frac{\partial \omega_0}{\partial \mu_1} \Big|_0 \Delta \mu_1 + \frac{\partial \omega_0}{\partial \mu_2} \Big|_0 \Delta \mu_2 \\
& + \frac{1}{2} \left[ \frac{\partial^2 \omega_0}{\partial T^2} \Big|_0 (\Delta T)^2 + \frac{\partial^2 \omega_0}{\partial \mu_1^2} \Big|_0 (\Delta \mu_1)^2 \right. \\
& + \left. \frac{\partial^2 \omega_0}{\partial \mu_2^2} \Big|_0 (\Delta \mu_2)^2 \right] + \frac{\partial^2 \omega_0}{\partial T \partial \mu_1} \Big|_0 \Delta T \Delta \mu_1 \\
& + \frac{\partial^2 \omega_0}{\partial T \partial \mu_2} \Big|_0 \Delta T \Delta \mu_2 + \frac{\partial^2 \omega_0}{\partial \mu_1 \partial \mu_2} \Big|_0 \Delta \mu_1 \Delta \mu_2,
\end{aligned} \tag{39}$$

where the subscript ‘‘0’’ after the partial derivatives and the ‘‘00’’ after  $\omega$  imply evaluation at  $T_0$ ,  $\mu_{01}$ , and  $\mu_{02}$ . The first term in the expansion is the actual Kramers free energy evaluated at  $T_0$  and  $\mu_{0i}$ , which is continuous at the interface if  $T_0$  and the  $\mu_{0i}$  correspond to equilibrium at a planar interface. The next three terms are individually zero, because  $de = Tds + \mu_1 dc_1 + \mu_2 dc_2$ , and because the derivatives are evaluated at  $T_0$ ,  $\mu_{01}$ , and  $\mu_{02}$ . The remaining terms can be computed from thermodynamic identities, and after some simplification, Eq. (39) can be rewritten

$$\begin{aligned}
\omega_0 = & \omega_{00} + \frac{1}{2} \left[ \frac{\partial s}{\partial T} \Big|_0 \Delta T^2 + \frac{\partial c_1}{\partial \mu_1} \Big|_0 \Delta \mu_1^2 + \frac{\partial c_2}{\partial \mu_2} \Big|_0 \Delta \mu_2^2 \right] \\
& + \frac{\partial c_1}{\partial T} \Big|_0 \Delta T \Delta \mu_1 + \frac{\partial c_2}{\partial T} \Big|_0 \Delta T \Delta \mu_2 + \frac{\partial c_1}{\partial \mu_2} \Big|_0 \Delta \mu_1 \Delta \mu_2.
\end{aligned} \tag{40}$$

Combining the three terms in Eq. (40) that contain derivatives with respect to the  $\mu_i$ , applying the condition that  $c_1 + c_2$  is constant, substituting  $dc = dc_2 = -dc_1$  and  $\mu = \mu_2 - \mu_1$  into Eq. (40), and using the relations  $\partial c / \partial \mu_1 = \partial c / \partial \mu$  and  $\partial c / \partial \mu_2 = -\partial c / \partial \mu$ , one obtains

$$\begin{aligned}
\frac{1}{2} \frac{\partial c_1}{\partial \mu_1} \Big|_0 (\Delta \mu_1)^2 + \frac{1}{2} \frac{\partial c_2}{\partial \mu_2} \Big|_0 (\Delta \mu_2)^2 + \frac{\partial c_1}{\partial \mu_2} \Big|_0 \Delta \mu_1 \Delta \mu_2 \\
= \frac{1}{2} \frac{\partial c}{\partial \mu} \Big|_0 (\Delta \mu)^2
\end{aligned} \tag{41}$$

and

$$\frac{\partial c_1}{\partial T} \Big|_0 \Delta T \Delta \mu_1 + \frac{\partial c_2}{\partial T} \Big|_0 \Delta T \Delta \mu_2 = \frac{\partial c}{\partial T} \Big|_0 \Delta T \Delta \mu, \tag{42}$$

where  $\Delta \mu = \mu - \mu_0$  and  $\mu_0 = \mu_{02} - \mu_{01}$ .

Next, substitute Eq. (41) into Eq. (40), then use Eq. (33) to evaluate  $\partial c / \partial \mu = b$  and  $\partial c / \partial T = 0$  and note that  $\partial s / \partial T \Big|_0 = c_v / T_0$ , where  $c_v$  is the heat capacity per unit volume at constant  $\mu$ , to find

$$\omega_0(T, \mu) = \omega_{00} + \frac{1}{2} \left[ b (\Delta \mu)^2 + \frac{c_0}{T_0} (\Delta T)^2 \right]. \tag{43}$$

By defining  $u = (\mu - \mu_0) / (\Delta c_0 / b)$  and  $\tilde{u} = (T - T_0) [c_v / (T_0 \mathcal{E}')]^{1/2}$ , where  $\mathcal{E}' = \Delta c_0^2 / b$ , Eq. (43) becomes

$$\omega_0(T, \mu) = \omega_{00} + \frac{1}{2} \mathcal{E}' [u^2 + \tilde{u}^2]. \tag{44}$$

Multiplying Eq. (12) by  $T_0$ , Eq. (28) by  $\mu_{0i}$ , and subtracting them from Eq. (8), one obtains

$$\begin{aligned}
\frac{d}{dt} \left[ \int_V \omega_0 dV + \int_{A^{S,L}} \omega_0^{xs} dA \right] = & - \int_{A_{\text{out}}} (\mathbf{j}_e - T_0 \mathbf{j}_s - \mu_0 \mathbf{j}) \cdot \mathbf{n} dA \\
& - T_0 \left[ \int_V \tilde{s}_I dV + \int_{A_{SL}} \tilde{s}_I^{xs} dA \right],
\end{aligned} \tag{45}$$

where  $V = V_S + V_L$ . One can apply Eq. (45) over a small time interval  $\Delta t$  and to a small volume  $V$  which, however, is sufficiently large that  $\mathbf{j}_e = \mathbf{0}$ ,  $\mathbf{j}_s = \mathbf{0}$ , and  $\mathbf{j} = \mathbf{j}_2 = \mathbf{0}$  on  $A_{\text{out}}$ .

Substituting  $\omega_0$  from Eq. (44) and noting that  $\tilde{s}_I$  and  $\tilde{s}_I^{xs}$  must be positive, one finds

$$\frac{d}{dt} \left\{ \int_V f dV + \int_{A_{SL}} f^{xs} dA \right\} \leq 0, \tag{46}$$

where

$$f = \frac{1}{2} [u^2 + \tilde{u}^2]$$

and

$$f^{xs} = \omega_0^{xs} / \mathcal{E}'.$$

## 2. Linear objective function

By multiplying Eq. (32) by  $\mu$ , multiplying Eq. (15) by  $T$ , and subtracting these from Eq. (11), one obtains

$$[\omega^S - \omega^L + (\omega^{xs} + \omega_{\theta\theta}^{xs}) K] V_n = -T \tilde{s}_I^{xs}, \tag{47}$$

where  $\omega^{xs}$  is assumed not to depend explicitly on time.

Integrating Eq. (47) over  $A_{S,L}$ , one finds

$$\begin{aligned}
\int_{A_{S,L}} (\omega^S - \omega^L) V_n dA + \int_{A_{S,L}} [\omega^{xs} + \omega_{\theta\theta}^{xs}] K V_n dA \\
= - \int_{A_{S,L}} T \tilde{s}_I^{xs} dA.
\end{aligned} \tag{48}$$

The Kramers free energy has as independent variables  $T$ ,  $\mu_1$ , and  $\mu_2$ . Expanding this free energy about some  $T_0$ ,  $\mu_{01}$ , and  $\mu_{02}$  to first order in the variables  $T$ ,  $\mu_1$ , and  $\mu_2$ , one finds for each phase ( $S$  or  $L$ ),

$$\begin{aligned}
\omega(T, \mu_1, \mu_2) = & \omega_{00} - s_0 (T - T_0) - c_{01} (\mu_1 - \mu_{01}) \\
& - c_{02} (\mu_2 - \mu_{02}),
\end{aligned} \tag{49}$$

where the subscript 0 on  $c$  and  $s$  and the subscript 00 on  $\omega$  indicate evaluation at  $T_0$ ,  $\mu_{01}$ , and  $\mu_{02}$ .

Choosing the variables  $T_0$ ,  $\mu_{01}$ , and  $\mu_{02}$  in solid and liquid to correspond to values for a flat interface at the melting point leads to  $\omega_{00}^S = \omega_{00}^L$  and

$$\Delta \omega := \omega^S - \omega^L = \Delta s_0 (T - T_0) + \Delta c_0 (\mu - \mu_0), \tag{50}$$

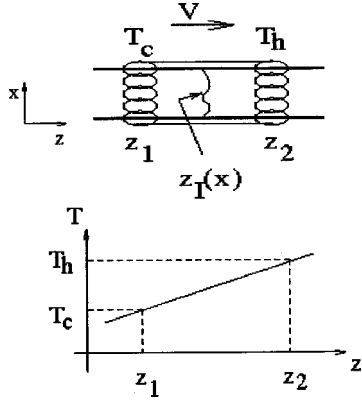


FIG. 2. The frozen temperature approximation for directional solidification. If the thermal diffusion coefficients in solid and liquid are large, and approximately equal, and if the latent heat of fusion is negligible, then the temperature field is constant in time and approximately linear in space in a reference frame that is moving at velocity  $\tilde{V}$  in the  $z$  direction. The interface is located at  $z_I$  somewhere between the thermal reservoirs, which maintain boundary conditions  $T_h$  and  $T_c$ .

where  $\mu_1^S = \mu_1^L$  and  $\mu_2^S = \mu_2^L$  at the interface and where  $\Delta s_0 = s_0^L - s_0^S$ ,  $\Delta c_0 = c_0^L - c_0^S$ . The definitions  $c := c_2$  and  $\mu := \mu_2 - \mu_1$  still hold, and so the definition  $\mu_0 = \mu_{02} - \mu_{01}$  has been used.

Consider the identity

$$\int_{A_{S,L}} \Delta \omega V_n dA = \frac{1}{2} \frac{d}{dt} \left[ \int_{V_S} \Delta \omega dV - \int_{V_{LK}} \Delta \omega dV \right] - \frac{1}{2} \left[ \int_{V_S} \frac{\partial}{\partial t} \Delta \omega dV - \int_{V_L} \frac{\partial}{\partial t} \Delta \omega dV \right]. \quad (51)$$

By the same reasoning presented in Sec. II to neglect a similar pair of integrals, and because it has been assumed for this model that the diffusion coefficients in solid and liquid are equal, the third and fourth integrals on the right-hand side of Eq. (51) sum to zero in the limit of small  $V$ .

Equation (51) can be substituted into Eq. (48) to give

$$\frac{d}{dt} \left[ \frac{1}{2} \int_{V_S} \Delta \omega dV - \frac{1}{2} \int_{V_L} \Delta \omega dV + \int_{A_{S,L}} \omega^{xs} dA \right] \approx - \int_{A_{S,L}} T \tilde{s}_I^{xs} dA. \quad (52)$$

The time derivative could be extracted from the second term in Eq. (48) to obtain Eq. (52) because we have assumed that  $\omega^{xs}$  does not depend explicitly on time.

Substituting Eq. (50) into Eq. (52) and defining

$$u := \frac{b}{\Delta c_0} (\mu - \mu_0), \quad (53)$$

$$\tilde{u}(T) := - \frac{\Delta s_0}{\mathcal{E}'} (T - T_0) = \frac{1}{m \Delta c_0} (T - T_0), \quad (54)$$

one obtains approximately the inequality (6), where

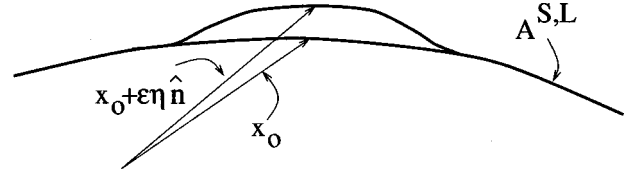


FIG. 3. Variation of interface position. The unperturbed interface position is identified by the points  $\mathbf{x}_0$ . This interface is perturbed to a position  $\mathbf{x}_0 + \epsilon \eta \mathbf{n}$ . Then the variational derivative of  $\mathcal{F}$  is computed to find the minimum.

$$f = \begin{cases} (u - \tilde{u})/2 & \text{in solid} \\ -(u - \tilde{u})/2 & \text{in liquid,} \end{cases} \quad (55)$$

and  $f^{xs} = \omega^{xs} / \mathcal{E}'$ .

In addition to the inequality (6), material is conserved. By substitution of  $c$  from Eq. (33) into Eq. (28), one finds that the conservation condition for material can be written in the form of Eq. (7) where it has been assumed that  $\mathbf{j} = \mathbf{0}$  on  $A_{\text{out}}$  and  $c_i^{xs} = 0$  as stated previously. An equation for the conservation of energy will not be written for this model because we will only treat the case of an isothermal system or use the frozen temperature approximation, which is described below.

For a coordinate system that is translating with speed  $\tilde{V}$  in the  $\hat{z}$  direction, lengths are rescaled by  $D/\tilde{V}$  and time by  $D/\tilde{V}^2$  to obtain Eq. (2) for the bulk diffusion equation.

### C. The frozen temperature approximation

The frozen temperature approximation can be used [18,20–22] to model directional solidification of a binary mixture. The temperature field is assumed to have a constant gradient  $\tilde{G}$  in the  $z$  direction, and to be translating at speed  $\tilde{V}$  in the  $z$  direction. In the moving reference frame, the temperature field is, therefore, constant in time.

The experimental setup in the directional growth geometry is sketched in Fig. 2. A heat source in advance of the domain of interest and a heat sink behind the domain of interest translate uniformly with respect to the sample at speed  $\tilde{V}$ . The heat source and sink are arranged so that the solidification front is located somewhere between them.

The temperature field can thus be written  $T(z) = \tilde{G}(\tilde{z} - \tilde{z}_0) + T_0$ , where  $\tilde{z}$  and  $\tilde{z}_0$  are dimensional lengths  $zD/\tilde{V}$  and  $z_0D/\tilde{V}$ . The value of  $\tilde{u}$  in Eq. (54) can thus be written

$$\tilde{u} = - \frac{\Delta s_0 \tilde{G} D}{\mathcal{E}' \tilde{V}} (z - z_0) = M(z - z_0), \quad (56)$$

where

$$M = \Delta s_0 \tilde{G} D / (\mathcal{E}' \tilde{V}) = \tilde{G} D / (m \Delta c_0 \tilde{V}). \quad (57)$$

In this approximation, the temperature field is legislated and the only field that must be computed is the compositional, or chemical potential, field. One could relax the frozen temperature condition in the variational model, and then one would also need to solve Eq. (1) for the temperature field. In this model, the only effect that the fixed temperature



field has on the computation is that it changes the interfacial boundary condition for the compositional field.

The frozen temperature approximation is a reasonable approximation that greatly simplifies calculations of directional solidification shapes, and includes enough of the important physics to display complex cellular morphologies similar to those observed in experiments. In particular, the parameter  $M$  is recognized to be precisely the bifurcation parameter that enters morphological stability theory for the limiting case of constitutional supercooling [23].

#### D. Correspondence between variational and standard sharp interface models

We choose a reasonable scheme for distributing the released heat or solute due to motion of the interface, and demonstrate that in the limit of small  $\Delta t$ , the boundary conditions maintained by the variational model are the same as those that are imposed in the standard sharp interface model.

The conservation condition, Eq. (7), that constrains the minimization in the variational model, is not specific about how the released potential from the moving interface should be distributed into the volume  $V$ . A sensible way of distributing the latent heat in the case of a pure material was suggested previously [7] and will be used here.

A minimization step is used to update the interface position from time  $t$  to time  $t + \Delta t$ , where  $\Delta t$  is a small time interval. The motion of the interface  $V_n \Delta t$  will bring about a change in the potential  $u$  in the neighborhood of the moving interface according to Eq. (7). Assuming that the distribution of the released heat or solute is determined by the diffusion equation, the maximum distance that the released potential can diffuse is of the order of  $\sqrt{\Delta t}$ .

A heat kernel can be used to compute the change in the potential field resulting from interface motion. The interface is a source of magnitude  $V_n \Delta t$ , so the change in chemical potential at  $\mathbf{x}_2$  can be computed from

$$\Delta u(\mathbf{x}_2) = \int_{A^{s,L}} G(|\mathbf{x}_1 - \mathbf{x}_2|, \Delta t) V_n(\mathbf{x}_1) \Delta t d\mathbf{x}_1, \quad (58)$$

where the function

$$G(|\mathbf{x}_1 - \mathbf{x}_2|, \Delta t) = (4\pi\Delta t)^{-(n/2)} \exp\left[-\frac{|\mathbf{x}_1 - \mathbf{x}_2|^2}{4\Delta t}\right] \quad (59)$$

is a heat kernel, and  $n$  is the dimensionality of the space. One can verify that this choice of  $\Delta u$  satisfies Eq. (7) by integrating Eq. (58) over the volume, and observing that  $G$  is normalized to one.  $\Delta u$  is negligible for  $|\mathbf{x}_1 - \mathbf{x}_2| > 2\sqrt{\Delta t}$ . Therefore, the volume  $V$  that is affected by the motion of the interface is small, for small  $\Delta t$ .

By choosing a configuration of the interface and allowing a local normal variation of that configuration near a point  $\mathbf{x}_0$  (see Fig. 3) one can compute a variation in  $\mathcal{F}$ , subject to conservation of energy in the form (58). One can determine the actual interfacial configuration by setting the variation equal to zero, which will be true when  $\mathcal{F}$  is a minimum. Then, the boundary condition in the limit can be determined by taking the limit of this configuration as  $\Delta t$  approaches zero.

The interface position will be identified by  $\mathbf{x}_0$  and the interface configuration by  $\mathbf{x}_0 + \epsilon \eta \mathbf{n}$ , where  $\eta$  is a function defined on  $\mathbf{x}_0$ ,  $\mathbf{n}$  is the unit normal vector pointing into the liquid, and  $\epsilon$  is a small parameter. The variation  $\delta\mathcal{F}$  using the linear form for  $f$  given in Eq. (25), can be computed as follows:

$$\delta\mathcal{F} = \delta \int_V f dV + \delta \int_{A^{s,L}} f^{xs} dA. \quad (60)$$

Evaluating the volume part of this variation first, one finds

$$\begin{aligned} \delta \int_V f dV &= \frac{1}{2} \left[ \int_{V^s} \delta(u - \bar{u}) dV - \int_{V^L} \delta(u - \bar{u}) dV \right. \\ &\quad \left. + \int_{A^{s,L}} (u - \bar{u}) \epsilon \eta dA \right. \\ &= \frac{1}{2} \left\{ \int_{V^s} \left[ \int_{A^{s,L}} G \epsilon \eta dA \right] dV \right. \\ &\quad \left. - \int_{V^L} \left[ \int_{A^{s,L}} G \epsilon \eta dA \right] dV \right\} \\ &\quad \left. + \int_{A^{s,L}} [(u - \bar{u})] \epsilon \eta dA, \right. \end{aligned} \quad (61)$$

where  $dA$  is a differential element of area. The second term in Eq. (60) can be computed to be

$$\delta \int_{A^{s,L}} f^{xs} dA = \int_{A^{s,L}} (f^{xs} + f_{\theta\theta}^{xs}) \epsilon \eta K dA, \quad (62)$$

where it has been assumed that  $f^{xs}(\theta)$  does not change explicitly during the variation. In the limit as  $\Delta t \rightarrow 0$ , the range of  $G$  becomes small compared to the radius of curvature of the interface, and the volume integrals in Eq. (61) cancel. Setting  $\delta\mathcal{F} = 0$  to find the minimum configuration, one finds

$$u - \bar{u} = -(f^{xs} + f_{\theta\theta}^{xs}) K, \quad (63)$$

which is the Gibbs-Thomson condition, Eq. (3), as it is written for the standard sharp interface model. Therefore, for small  $\Delta t$ , the two models should give similar results. Variational simulations have been tested by showing that the simulation produces solutions that agree with some analytical solutions found by solving standard sharp interface models. A simulation [24] of the process of directional solidification using the vibrational algorithm predicted the critical conditions for morphological stability that agree with analytical solutions for the critical conditions calculated from sharp interface models [23]. In another implementation of a variational simulation, parabolic dendrites were computed for which the tip curvatures and Peclet numbers agreed with the values predicted by Ivantsov [25].

## IV. CONCLUSIONS

In this paper, variational models for solidification are derived by using the principles of nonequilibrium thermodynamics. Laws of conservation and entropy production lead to the equations that are summarized in Sec. I. Variational prin-

principles are obtained for two different physical systems: the free growth of a pure material into a supercooled melt, and the directional solidification of a binary mixture. In both cases, two different expressions for the relevant free-energy density are found: a quadratic form, and a linear form. The quadratic form does not require the neglect of terms such as the second term in Eq. (26), and is also associated with a global minimizer for the entire variational algorithm. Variational models had been used previously on the basis of their mathematical connection to standard sharp interface models. The derivations that are presented here provide a direct link between those models and irreversible thermodynamics.

These variational models provide an alternative approach for modeling the process of solidification. Several modeling assumptions that can limit their applicability were necessary. The system is assumed to be symmetric in that the transport coefficients are equal in solid and liquid. For thermal transport this is reasonable, but for the diffusion of material, this approximation is inappropriate in most cases. The frozen

temperature approximation can be used to simplify the calculation for the binary mixture.

A computational advantage of the variational approach over standard sharp interface model is that the curvature does not need to be computed directly. Using a simulation based on the variational model [7,24], one can employ relatively coarse meshes to compute the evolution of crystal shapes. Another advantage is that the variational approach incorporates thermodynamic laws more directly through the minimization of an energy, as opposed to assigning a boundary condition whose value was determined separately by such a minimization.

#### ACKNOWLEDGMENTS

The authors would like to acknowledge funding from the National Science Foundation under Grant Nos. DMR-9211276 and DMR-9634056. R.A. was supported by NSF Career Grant No. DMS-9502059.

- 
- [1] S. L. Wang *et al.*, *Physica D* **69**, 189 (1993).
  - [2] A. A. Wheeler, W. J. Boettinger, and G. B. McFadden, *Phys. Rev. A* **45**, 7424 (1992).
  - [3] A. A. Wheeler, B. T. Murray, and R. J. Schaefer, *Physica D* **66**, 243 (1993).
  - [4] G. Caginalp and W. Xie, *Phys. Rev. E* **48**, 1897 (1993).
  - [5] R. Kobayashi, *Bull. Jpn. Soc. Ind. Appl. Math* **1**, 22 (1991).
  - [6] H. M. Sonner, *Arch. Ration. Mech. Anal.* **131**, 139 (1995).
  - [7] R. Almgren, *J. Compu. Phys.* **106**, 337 (1993).
  - [8] A. Roosen and J. Taylor, *J. Comput. Phys.* **114**, 113 (1994).
  - [9] J. Taylor, *Bull. Am. Math. Soc.* **84**, 568 (1978).
  - [10] J. Taylor, *Acta Metall. Mater.* **40**, 1475 (1992).
  - [11] J. Taylor, *SIAM J. Control Optim.* **31**, 387 (1993).
  - [12] W. H. Giedt, *Principals of Engineering Heat Transfer* (Van Nostrand Co., Princeton, 1957).
  - [13] F. Melo and P. Oswald, *Phys. Rev. E* **47**, 2654 (1993).
  - [14] S. Angenent and M. E. Gurtin, *Arch. Ration. Mech. Anal.* **104**, 195 (1988).
  - [15] S. Angenent and M. E. Gurtin, *Arch. Ration. Mech. Anal.* **108**, 324 (1989).
  - [16] B. K. Johnson and R. F. Sekerka, *Phys. Rev. E* **52**, 6404 (1995).
  - [17] F. Almgren, J. Taylor, and L. Wang, *SIAM J. Control Optim.* **31**, 387 (1993).
  - [18] J. S. Langer, *Rev. Mod. Phys.* **52**, 1 (1980).
  - [19] R. F. Sekerka and W. W. Mullins, *J. Chem. Phys.* **73**, 1413 (1980).
  - [20] J. S. Langer and L. A. Turski, *Acta Metall.* **25**, 1113 (1977).
  - [21] K. Brattkus and S. H. Davis, *Phys. Rev. B* **38**, 11 452 (1988).
  - [22] J. Vinals, R. F. Sekerka, and P. P. Debroy, *J. Cryst. Growth* **89**, 405 (1988).
  - [23] R. F. Sekerka, *Phase Interfaces: Morphological stability*, in *Encyclopedia of Materials Science and Engineering*, edited by Michael B. Bever (Pergamon Press Ltd., Oxford, 1986).
  - [24] B. K. Johnson, Ph.D. thesis, Carnegie Mellon University, 1996.
  - [25] G. P. Ivantsov, *Dokl. Akad. Nauk. SSSR* **58**, 567 (1947).